Chen *et al.*
Protection and Control of Modern Power Systems (2023) 8:2
https://doi.org/10.1186/s41601-022-00275-6

Protection and Control of Modern Power Systems

ORIGINAL RESEARCH Open Access

Optimal layout model of feeder automation equipment oriented to the type of fault detection and local action

Ruizhi Chen[1*], Xihong Li[1] and Yanbo Chen[2]

Abstract

In feeder automation transformation there are difficulties in equipment and location selection. To help with this, an optimal layout model of feeder automation equipment oriented to the type of fault detection and local action is proposed. It analyzes the coordination relationship of the three most common types of automation equipment, i.e., fault indicator, over-current trip switch and non-voltage trip switch in the fault handling process, and the explicit expressions of power outage time caused by a fault on different layouts of the above three types of equipment are given. Given constraints of power supply reliability and the goal of minimizing the sum of equipment-related capital investment and power interruption cost, a mixed-integer quadratic programming model for optimal layout is established, in which the functional failure probability of equipment is linearized using the 3δ principle in statistics. Finally, the basic characteristics of the proposed model are illustrated by different scenarios on the IEEE RBTS-BUS6 system. It can not only take into account fault location and fault isolation to enhance user power consumption perception, but also can guide precise investment to improve the operational quality and efficiency of a power company.

Keywords: Feeder automation, Equipment layout optimization, Power outage time, Explicit expression, Mixed integer quadratic programming model, Functional failure probability of equipment

1 Introduction

Faults in a power system mainly occur in the distribution network, and these faults can seriously affect customer power consumption perception [1–3]. The use of feeder automation technology can reduce the negative impact of faults and improve the satisfaction of electricity consumers [4, 5]. The main feature of feeder automation is that when permanent faults causing power outage on a distribution network, then if suitable distribution automation equipment is installed in a suitable location, the equipment can locate the faults from fault current information, and isolate the faults. Consequently, the power supply of the load that is not in a faulty area can be restored quickly. Looking at the different functions in this process, distribution automation equipment can be divided into type of fault detection and type of fault isolation.

The main type of fault detection equipment is the fault indicator, which detects the fault current flowing through itself and sends a signal to the distribution main-station through GPRS, thereby helping the distribution main-station to locate the fault.

Switches are the main types of fault isolation equipment. Depending on the type of switch action, it can be further divided into centralized control and local action. For the former, the distribution main-station is connected to it through an optical fiber for remote control, namely, a remote control switch. For the latter, there is no optic connection to the distribution main-station, so if the electrical signals it collects reach preset thresholds, it will act on its own. Examples are the overcurrent and non-voltage trip switches, abbreviated to I-type switch

*Correspondence: 2169889956@qq.com

[1] Bishan Power Supply Branch of Chongqing Electric Power Company, Chongqing, Bishan, China
Full list of author information is available at the end of the article

and V-type switch in this paper, respectively. However, most V-type switches will be equipped with communication modules for communication with the distribution main-station through GRPS, so it also has the function of fault location. It is worth noting that for safety reasons, the remote control command of the switch must go through optical fiber, so a V-type switch is usually not suitable for remote control.

Because of complex topology and uneven load distribution on a network it is impossible to intuitively determine installation location and type of distribution automation equipment. Having too many installations will significantly increase the operating cost, while too few will not ensure reliable power supply. How to reasonably configure feeder automation equipment to effectively accelerate fault location, fault isolation and service restore (FLSR) is a hot issue in the process of feeder automation transformation [6]. In particular, the remote control switch can greatly improve power supply reliability because it can be controlled by humans, thereby reducing the possibility of wrong action and refusal of action. However, because of reasons such as capital investment, fiber channel and maintenance level constraints, I-type and V-type switches are more commonly used [7].

Reference [8] proposes a fault identification and localization method based on data acquisition and monitoring of the distribution network, and uses a fuzzy Petri net. References [9–11] consider the role of fault indicators in the line patrol process, and propose a distribution network reliability evaluation model based on fault information variables, and determine its optimal configuration to meet reliability requirements and improve the fault location capability. Intelligent algorithms can easily fall into local optima or have slow convergence. Thus in [12, 13], based on an algebraic operation relationship, using a nonlogical modeling method to describe the approximation relationship of fault location in the network is proposed, and a fault location model with high tolerance performance is constructed. For fault isolation, reference [14] studies the power outage time with different expected faults and proposes a distribution network reliability evaluation method for feeder automation, and it further establishes an equipment-related capital investment and optimization model with the goal of minimizing the sum of power outage costs caused by faults. In [15], the feeder is divided into different base segments according to user information, in which the feeder relationship matrix is determined according to equipment position. Equipment layout results are obtained by substituting the relevant parameters of fault handling. In [16, 17], the influence of low probability extreme weather is considered. This improves the robustness of equipment layout results. Reference [18] uses a defense-attack-defense framework to improve the service recovery ability of a distribution network under severe faults. The V-type switch layout problem in [19] is modelled as a mixed-integer nonlinear programming problem, which aims to minimize the total cost with the reliability index of average service available index as the constraint. Reference [20] describes a general index of single switches for fault location, and sets constraints such as to maximize the improvement effect of the index and switch cost, and proposes a three-stage optimization algorithm for the configuration of medium voltage overhead line switches. Reference [21] uses an efficient graph search algorithm combined with a directed graph of the network to preprocess network data and improve the efficiency of the planning model solution.

Reference [22] studies the optimal amount of equipment from the perspective of input and output, and puts forward a differentiation design principle of equipment configuration according to different types of power distribution area. References [23, 24] propose a two-stage optimization method to solve the problem through a heuristic algorithm. Among them, the function of feeder automation equipment is mainly to accelerate fault location and isolation. In [25, 26], a planning model of a fault indicator and V-type switch is established considering the influence of reliability and economy reconfiguration.

However, the above research rarely studies the cooperative relationship of fault indicator, I-type switch and V-type switch in the fault handling process, and seldomly considers the functional failure probability of equipment. At the same time, the expression of power outage time is not intuitive, and most developed models are non-convex models, whose solution quality is relatively low. To overcome the above shortcomings, an optimal layout model of feeder automation equipment oriented to the type of fault detection and local action is proposed. The main contributions of this paper are:

(1) The cooperative relationship of fault indicator, I-type switch and V-type switch in the FLSR process is analyzed.
(2) Based on (1), an explicit expression of power outage time with equipment layout is built, and then the equipment layout optimization model is developed.
(3) We linearize power outage time and functional failure probability of equipment in (2), then convert the model to a mixed integer quadratic programming model while fitting the actual production situation as much as possible to ensure a global optimal solution.
(4) Finally, using a variety of scenarios, it is verified that the proposed model can efficiently solve the optimal layout problem of multi-type equipment, and

maintain a balance between reliability and economy, suitable for engineering application.

In order to further highlight the advantages of the proposed model, its features are compared with other similar studies in Table 1.

2 Mathematical model

2.1 Problem statement

The key to solving the problem of optimal layout of feeder automation equipment is to describe the relationship between the power outage time caused by a specific fault with specific equipment layout through reasonable mathematical language. Figure 1 illustrates the cooperation of fault indicator, I-type switch and V-type switch in the FLSR process.

The feeder in Fig. 1 has poles No. 1 to No. 4 which connect to load area j_1 to j_4, respectively. There is a normally closed breaker at the outlet of the line, and a normally open tie switch for load transfer at the end of line. For feeder automation equipment, its configuration position is generally on both sides of a pole. Under normal conditions, the entire line load is powered by the substation breaker.

Assuming that a permanent fault occurs in the T-connected line where load area j_3 is located, in order to reduce the impact of transient faults, the FLSR process is mainly divided into four stages as follows.

Stage 1: Overcurrent protection of the nearest I-type switch upstream of the fault will trip, and the downstream load area will lose power at the same time. All the corresponding V-type switches will be opened because of voltage disappearance, while the tie switch will detect voltage disappearance on one side and start timing for closing. Fault current flows through the V-type switch on the No. 2 pole, but does not flow through the fault indicator. Therefore, the dispatch center judges that the fault occurs in the line between No. 2 pole and No. 3 pole, and the T-connected line in No. 3 pole according to the signal.

Table 1 Feature comparison of different models

Feature	[8]	[9–11]	[12–18]	[19, 20]	[21]	[22–24]	[25, 26]	Proposed model
I	√	√				√	√	√
II					√			√
III			√	√	√	√	√	√
IV		√	√		√		√	√
V								√

I: Fault indicator is considered for installation. II: I-type switch is considered for installation. III: V-type switch is considered for installation. IV: The global optimal solution can be obtained. V: Considering functional failure probability

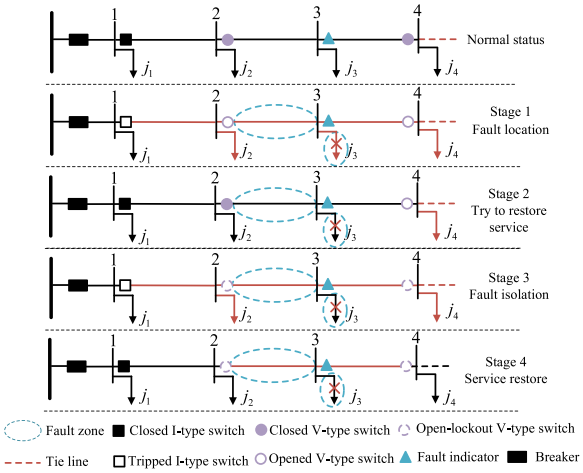

Fig. 1 FLSR process

Stage 2: The tripped I-type switch is reclosed for the first time and the downstream V-type switch is reclosed after a delay, in an attempt to deliver power segment by segment, so as to eliminate power outage caused by the transient fault. At the same time, the two nearest V-type switches upstream and downstream of the fault both detect voltage.

Stage 3: Since the fault still exists, the I-type switch is tripped for the second time because of overcurrent protection action, and the downstream V-type switch opens again. The two nearest V-type switches upstream and downstream of the fault have open-lockout to isolate the fault because the time for detecting voltage has not reached the fixed value.

Stage 4: The tripped I-type switch is reclosed for the second time to restore power supply to the non-fault area. The tie switch automatically closes after the one-side voltage loss reaches a fixed value and the downstream non-fault area restores power supply segment by segment. For the load in the fault area, the power supply can only be restored after the line patrol has found the fault and carried out the repair.

In summary, the three types of automation equipment jointly determine power outage time $T_{i,j}^{\text{outage}}$ of the load point j caused by fault i, and can be divided into the following three categories:

$$T_{i,j}^{\text{outage}} = \begin{cases} 0 & j_1 \\ t^{\text{iso}} & j_2, j_4 \\ t^{\text{loc}} + T_i^{\text{patrol}} + t^{\text{rep}} & j_3 \end{cases} \tag{1}$$

where t^{loc} is the judgment time for fault location, t^{iso} is the operating time for the V-type switch, t^{rep} is the expected repair time for the fault, and T_i^{patrol} is the patrol time for fault i where this time is a variable related to the layout of the fault indicator and V-type switch.

This paper will build an explicit expression for the relationship between the layout of the feeder automation equipment and the power outage time around Eq. (1), and linearize the nonlinear terms involved, to obtain the optimal layout model of that can obtain a global optimal solution.

2.2 Patrol time

It can be seen from Fig. 1 that for any segment s of the feeder, as long as there is at least one fault indicator or V-type switch between itself and fault i, it is not necessary to patrol. From [25], we define the Boolean variable $b_{i,s}$. When its value is 0 this means the segment needs to be patrolled, and 1 means the patrol not needed. The formulae are:

$$X_{i,s} = \sum_{n \in \Omega_{i,s}} x_n \tag{2}$$

$$Z_{i,s} = \sum_{n \in \Omega_{i,s}} z_n \tag{3}$$

$$\frac{X_{i,s} + Z_{i,s}}{M} \le b_{i,s} \le X_{i,s} + Z_{i,s} \tag{4}$$

where x_n and z_n represent the Boolean configuration variable of the fault indicator and V-type switch corresponding to the nth configuration position on the feeder. When its value is 1 this indicates that the corresponding equipment is configured at the corresponding position, and when 0 it indicates that it has not been configured. $\Omega_{i,s}$ is the set of configuration positions between fault i and segment s. $X_{i,s}$ and $Z_{i,s}$ are the quantity of fault indicator and V-type switch corresponding to $\Omega_{i,s}$. M is a maximum value, which is taken as 1000 in this paper. From Eq. (4), it can be seen that as long as there is at least one fault indicator or V-type switch in $\Omega_{i,s}$, $b_{i,s}$ will equal 1, which means that the line segment s does not need to be patrolled. Because the fault indicator and V-type switch generally use GRPS to communicate, there is a functional failure probability of communication. Thus, the patrol time for fault i is further established as:

$$t_{i,s}^{\text{search}} = \frac{l_s}{v} \times \left(1 - \left(1 - \rho_{i,s}\right) \times b_{i,s}\right) \tag{5}$$

$$T_i^{\text{patrol}} = \sum_{s \in \Omega_s} t_{i,s}^{\text{patrol}} \tag{6}$$

where $t_{i,s}^{\text{patrol}}$ is the expected patrol time of segment s for fault i. l_s is the length of segment s, v is the patrol speed, and $\rho_{i,s}$ is the probability that all communication functions of the fault indicators and V-switches between fault i and line s fail at the same time. Ω_s is the segment set of the feeder.

$\rho_{i,s}$ should be an exponential function with the functional failure probability of single equipment as the base, and the quantity of equipment between fault i and line s as the index, representing the probability of simultaneous functional failure of all equipment between fault i and line s. Although it can be linearized by Taylor expansion, the error of low-order expansion is significant, whereas high-order expansion will bring too many additional terms. Therefore, the 3δ principle in statistics is introduced. The specific method is to consider that the functional failure probability decreases exponentially with the increase of quantity of equipment, but after it becomes less than 0.0027, it no longer changes. Thus, it transforms the exponential function into a piecewise function, as shown in Fig. 2, in which the functional failure probability of a single piece of equipment is 0.2.

For the convenience of expression, the piecewise function is defined as:

$$\rho_{i,s} = f(\rho, X_{i,s} + Z_{i,s}) = \begin{cases} \rho^{X_{i,s}+Z_{i,s}} & X_{i,s} + Z_{i,s} < G \\ \rho^{G} & X_{i,s} + Z_{i,s} \ge G \end{cases} \tag{7}$$

where ρ is the functional failure probability of single equipment, G is the number of segments, and has the following value constraints:

$$\begin{cases} \rho^{G-1} \ge 0.0027 \\ \rho^{G} < 0.0027 \end{cases} \tag{8}$$

The piecewise function is implemented using a Special-Ordered Set of type 2, namely SOS2 constraints [14], as:

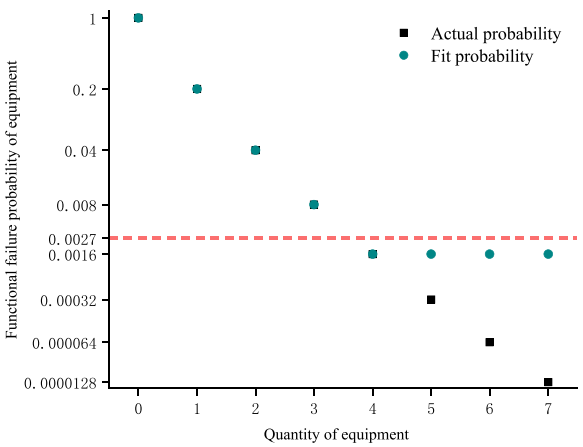

Fig. 2 Schematic diagram of functional failure probability

$$f(\rho, X_{i,s}+Z_{i,s}) = \sum_{g=1}^{G+1} \gamma(g) \times \rho(g) \tag{9}$$

$$\rho(g) = \begin{cases} p^g & g \le G \\ \rho^G & g = G+1 \end{cases} \tag{10}$$

$$\sum_{g=1}^{G+1} \gamma(g) \times \tau(g) = X_{i,s} + Z_{i,s} \tag{11}$$

$$\tau(g) = \begin{cases} g & g \le G \\ sum(\Omega_{i,s}) & g = G+1 \end{cases} \tag{12}$$

$$0 \le \gamma(g) \le 1 \quad 1 \le \forall g \le G+1 \tag{13}$$

$$\sum_{g=1}^{G+1} \gamma(g) = 1 \tag{14}$$

$$\gamma(g) \le b(g) \quad 1 \le \forall g \le G+1 \tag{15}$$

$$\sum_{g=1}^{G+1} b(g) \le 2 \tag{16}$$

$$\begin{cases} b(g) + b(g+\delta) \le 1 \\ 1 \le \forall g \le G+1 \\ 1 < \forall \delta \le G+1-g \end{cases} \tag{17}$$

where $\gamma(g)$ is the SOS2 coefficient corresponding to segment g, $\rho(g)$ is the failure probability corresponding to segment g, and $\tau(g)$ is the quantity of equipment corresponding to segment g. $b(g)$ is the auxiliary Boolean variable corresponding to segment g, $sum(\Omega_{i,s})$ is the quantity of elements in $\Omega_{i,s}$, and δ is the auxiliary integer variable.

Equations (15)–(17) show that in SOS2 constraint, $\gamma(g)$ can only take non-zero values at 1 or 2 segments, and the two segments must be continuous. The following is further illustrated by Fig. 3.

In Fig. 3, the functional failure probability of a single piece of equipment is 0.2, and the maximum number of pieces of equipment is 50. From the above assumption, when the number of pieces is fewer than or equal to 4, the probability decreases exponentially. Thus, G equals 4, and after there are more than four pieces the probability does not change. The continuous curve is divided into 5 segments, and the values of $\rho(g)$ and $\tau(g)$ are listed in Table 2.

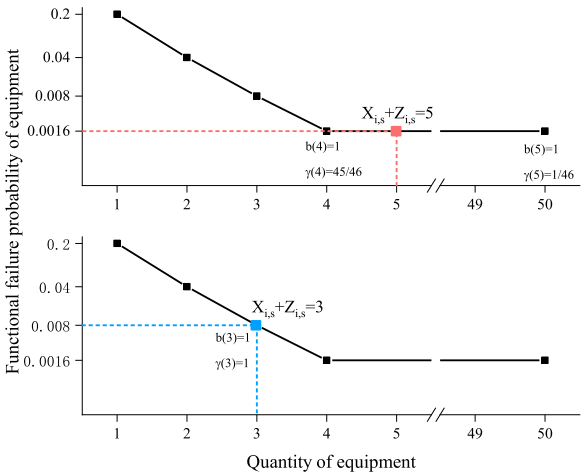

Fig. 3 Schematic diagram of SOS2 constraint

Table 2 Variable values

	$g=1$	$g=2$	$g=3$	$g=4$	$g=5$
$\rho(g)$	0.2	0.04	0.008	0.0016	0.0016
$\tau(g)$	1	2	3	4	50

According to the amount of equipment, it is divided into the following two cases:

(1) If the number of pieces is 5, between segment G and $G+1$, in order to satisfy Eq. (11), $b(4)$ and $b(5)$ are both equal to 1, $\tau(4)$ and $\tau(5)$ are 45/46 and 1/46, respectively. Substituting them into Eq. (9) obtains $f(0.2, 5)$ as 0.0016

(2) If the number of pieces is 3 and fewer than G, Eq. (11) is satisfied only if $b(3)$ is 1. As $\tau(3)$ is 1, $f(0.2, 3)$ is 0.008.

The piecewise functions involved in the following are all processed in the above manner.

In Eq. (5), there is a nonlinear term multiplied by a Boolean variable and a continuous variable. These can be linearized by the big-M method [18], as:

$$\frac{\nu}{l_s} \times t_{i,s}^{\text{patrol}} + (M-1) \times (b_{i,s}-1) \le \rho_{i,s} \tag{18}$$

$$\frac{\nu}{l_s} \times t_{i,s}^{\text{patrol}} + (1-M) \times (b_{i,s}-1) \ge \rho_{i,s} \tag{19}$$

$$\frac{\nu}{l_s} \times t_{i,s}^{\text{patrol}} + (1-M) \times b_{i,s} \le 1 \tag{20}$$

$$\frac{v}{l_s} \times t_{i,s}^{\text{patrol}} + (1+M) \times b_{i,s} \geq 1 \tag{21}$$

Similar nonlinear terms involved in the followings are also processed in the above manner.

2.3 Outage time

The FLSR process described in Fig. 2 is based on a linear distribution network, while load and fault can only be related to each other upstream and downstream. However, the actual distribution network structure is complex, as load and fault may be located in different branches under a public node. For the public node, if it cannot be isolated from the fault, it will be involved in a power outage, and this will indirectly lead to load power outage. In contrast, if there is at least one I-type switch on the path from the public node to the fault, the fault will be isolated directly from the path, without causing load power outage. Therefore, in order to establish the explicit expression of power outage time of automation equipment, $\Omega_{i,j}^{i}$ is defined as the set of configuration positions between the last public node of fault i and load j to fault i, whose schematic diagram is shown in Fig. 4.

There are three cases according to the location relationship between load j and fault i, as follows:

> Case 1: Load is downstream of the fault. For example, for load j_4, the fault between poles No. 1 and 2 is upstream and the fault location itself is the last public node, so $\Omega_{i,j}^{i}$ will be an empty set.
> Case 2: Load is upstream of the fault. For example, for load j_1, the fault between poles No. 2 and 4 is downstream. No. 1 pole is the public node, and the 2nd, 3rd and 6th configuration positions are in $\Omega_{i,j}^{i}$.
> Case 3: Load and fault are in different branches. For example, load j_4 and the fault between poles No. 2 and 3 are in different branches. No. 2 pole is the public node, and the 4th configuration position is in $\Omega_{i,j}^{i}$.

The I-type switch may not operate correctly because of improper parameter setting. However, as long as there is at least one V-type switch between the load and the fault, the outage time will not be longer than the fault isolation time. According to [25, 27], the power outage time $T_{i,j}^{\text{outage}}$ can be established as:

$$Y_{i,j}^{i} = \sum_{n \in \Omega_{i,j}^{i}} y_n \tag{22}$$

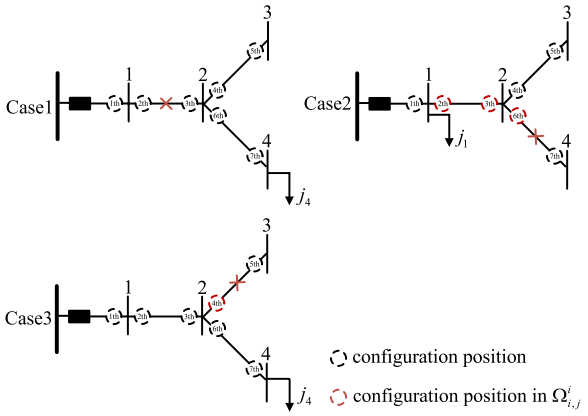

Fig. 4 Schematic diagram of $\Omega_{i,j}^{i}$

$$Z_{i,j} = \sum_{n \in \Omega_{i,j}} z_n \tag{23}$$

$$T_{i,j}^{\text{outage}} \geq f\left(\rho, Y_{i,j}^{i}\right) \times t^{\text{iso}} \tag{24}$$

$$T_{i,j}^{\text{outage}} \geq \left(1 - Y_{i,j}^{i}\right) \times t^{iso} \tag{25}$$

$$T_{i,j}^{\text{outage}} \geq \left(1 - Y_{i,j}^{i} - Z_{i,j}\right) \times \left(t^{\text{loc}} + T_{i}^{\text{search}} + t^{\text{repair}}\right) \tag{26}$$

where y_n represents the Boolean configuration variable of the I-type switch corresponding to the nth configuration position on the feeder. $Y_{i,j}^{i}$ is the number of I-type switches corresponding to $\Omega_{i,j}^{i}$, and $\Omega_{i,j}$ is the set of configuration positions between fault i and load j. $Z_{i,j}$ is the number of V-type switches corresponding to $\Omega_{i,j}$. $f\left(\rho, Y_{i,j}^{i}\right)$ is the functional failure probability of I-type switches corresponding to $\Omega_{i,j}^{i}$, and $f\left(\rho, Y_{i,j}^{i}\right)$ times t^{iso} represents the expected isolation time when all I-type switches in $\Omega_{i,j}^{i}$ fail.

The relationship between the power outage time and the automation equipment is described by the three inequalities from Eqs. (24)–(26). These are now explained in detail.

(1) If there is no I-type switch in $\Omega_{i,j}^{i}$ and no V-type switch in $\Omega_{i,j}$, in the mathematical sense, both $Y_{i,j}^{i}$ and $Z_{i,j}$ are equal to 0. Among the right terms of the three equations, the right term of Eq. (26) is the largest, which is the minimum value of $T_{i,j}^{\text{outage}}$. In a physical sense, it means that if the load cannot

be isolated from the fault by the I-type and V-type switches, at least it needs to wait for the main-station to roughly locate the fault, and then restore the power supply after searching for the actual fault location and carrying out repair.

(2) If there is no I-type switch in $\Omega_{i,j}^{i}$, but at least one V-type switch in $\Omega_{i,j}$, then similar to above, the minimum value of $T_{i,j}^{\text{outage}}$ is the right term of Eq. (25). It means that although the load cannot be isolated from the fault by the I-type switch without causing a power outage, it can still be isolated by the V-type switch and power supply can be quickly restored.

(3) As long as there is at least one I-type switch in $\Omega_{i,j}$, the minimum value of $T_{i,j}^{\text{outage}}$ is $f\left(\rho, Y_{i,j}^{i}\right)$ times t^{iso}.

In particular, if the optimization goal involves minimizing the derivative of the power outage time, such as a goal of minimizing the customer interrupt cost, it is desirable that the power outage time of any load under any fault should be as small as possible, around the minimum value that can be obtained. The power outage time in such a condition can be precisely expressed by the following explicit expression:

$$T_{i,j}^{\text{outage}} = \begin{cases} f\left(\rho, Y_{i,j}^{i}\right) \times t^{\text{iso}} & Y_{i,j}^{i} \geq 1 \\ t^{\text{iso}} & Y_{i,j}^{i} = 0, Z_{i,j} \geq 1 \\ t^{\text{loc}} + T_{i}^{\text{patrol}} + t^{\text{repair}} & Y_{i,j}^{i} + Z_{i,j} = 0 \end{cases} \tag{27}$$

2.4 Reliability index

To effectively help power companies to carry out distribution automation transformation, we improve the two main assessment indicators of the State Grid for a distribution network, namely the normal power supply time and the number of trips of a substation breaker.

Based on the above requirements, the average service availability index (ASAI) is used as one of the reliability indicators. This reflects the annual proportion of normal power supply through a percentage value, as:

$$\text{ASAI} = \left(1 - \frac{\sum_{i \in \Omega_i} \sum_{j \in \Omega_j} \lambda_i N_j T_{i,j}^{\text{outage}}}{8760 \times \sum_{j \in \Omega_j} N_j}\right) \times 100\% \tag{28}$$

where Ω_i is the set of faults, Ω_j is the set of loads. λ_i is the probability of fault i, and N_j is the quantity of users at load j. The number of hours in one year is 8760.

The system average interruption frequency index (SAIFI) for a breaker is used as another reliability indicator. This counts the annual expected number of trips of a breaker in a substation, as:

$$Y_i = \sum_{n \in \Omega_{i,0}} y_n \tag{29}$$

$$\frac{Y_i}{M} \leq b_i \leq Y_i \tag{30}$$

$$\text{SAIFI} = \sum_{i \in \Omega_i} \lambda_i \times \left(1 - b_i \times \left(1 - f(\rho, Y_i)\right)\right) \tag{31}$$

where $\Omega_{i,0}$ is the set of configuration positions between fault i and the substation breaker, and Y_i is the number of I-type switches corresponding to $\Omega_{i,0}$. b_i is the auxiliary Boolean variable used to judge whether there is an I-type switch in $\Omega_{i,0}$, and $f(\rho, Y_i)$ is the piecewise function of failure probability with respect to Y_i.

2.5 Economic indicators

In this paper, the equipment life cycle cost (*ELCC*) is used as one of the economic indicators. This includes the equipment installation and maintenance costs during the entire equipment life cycle, as:

$$ELCC = \left(\sum_{n \in \Omega_n} \left(x_n inv^{\text{F}} + y_n inv^{\text{I}} + z_n inv^{\text{V}}\right)\right) \left(1 + \sum_{t \in \Omega_t} \frac{1}{(1+DR)^t}\right) \tag{32}$$

where Ω_n is the set of all configuration positions on feeder. inv^{F}, inv^{I} and inv^{V} are the purchase and configuration costs of fault indicator, I-type switch and V-type switch, respectively. Ω_t is the service life of distribution automation equipment, and DR is the maintenance rate.

The customer interrupt cost (*CIC*) is used as the second economic index. This counts the electricity bills that cannot be received because of power outages during the entire equipment life cycle, and is given as:

$$CIC = \sum_{t \in \Omega_t} \sum_{i \in \Omega_i} \sum_{j \in \Omega_j} \sum_{k \in \Omega_{j,k}} \lambda_i T_{i,j}^{\text{outage}} P_{j,k} R_k (1+\mu)^t \tag{33}$$

where $\Omega_{j,k}$ is the set of all load types of load j, $P_{j,k}$ is the load power of the kth type load at load point j, R_k is electricity price of the kth type load, and μ is the average load growth rate.

2.6 Optimization layout model

In order to obtain the most reasonable equipment layout to meet the requirements of power supply reliability with the minimal economic investment, in this paper, two types of reliability indicators are used as constraints, and the sum of equipment life cycle cost and customer interrupt cost is minimized as the goal to build an optimal layout model of feeder automation equipment. Since both the fault indicator and V-type switch have communication function, and the I-type switch and V-type switch both have isolation function, repeated installation in the same position will cause a waste of money. Thus, the corresponding constraints, i.e., the same position cannot have two equipment with overlapping functions, are added. The model is given as:

$$\begin{aligned} &minimize\ ELCC + CIC \\ &s.t. \begin{cases} \mathrm{ASAI} \geq \mathrm{ASAI}^{\mathrm{lim}} \\ \mathrm{SAIFI} \leq \mathrm{SAIFI}^{\mathrm{lim}} \\ x_n + z_n \leq 1 \\ y_n + z_n \leq 1 \\ \forall n \in \Omega_n \end{cases} \end{aligned} \tag{34}$$

where $\mathrm{ASAI}^{\mathrm{lim}}$ is the lower limit of the reliability index ASAI. So the ASAI reliability of the model needs to be higher than this value. $\mathrm{SAIFI}^{\mathrm{lim}}$ is the upper limit of the reliability index SAIFI, so the SAIFI reliability of the model needs to be lower than this value.

3 Case study

In this paper, the No. 4 feeder of IEEE RBTS-BUS6 is used to test the validity and rationality of the above optimal layout model in different scenarios. The feeder has a total of 23 load points, 1138 users, and 49 configuration positions, while the average load is about 4.815 MW. The details on the line length, load, and number of users can be found in [28].

Some of the parameters are set as follows: patrol speed v is 1 m/s; equipment invalid rate ρ is 0.2 [27]; line failure probability λ_i is 0.065 times/km-year; inv^{F}, inv^{I} and inv^{V} are ¥5000, ¥30,000 and ¥60,000 respectively; equipment service life Ω_t is 5 years; maintenance rate DR and average load growth rate μ are both 0.05; electricity prices for residents, and industrial and commercial loads are ¥0.52/kWh, ¥0.64/kWh and ¥0.64/kWh, respectively; judgment time t^{loc} is 30 s; V-type switch operating time t^{iso} is 60 s; and expected repair time t^{repair} is 28800 s.

Given the above parameters without any equipment, the initial ASAI of the test feeder is 98.85%, the initial SAIFI is 4.01, and the initial CIC is ¥7,789,528.

To obtain the global optimal solution, the optimal layout model in this paper is constructed as a convex model. The following calculation examples are all written based on Python 3.8 and solved by branch and bound algorithm. The optimization gap is 0%. The computer used has a processor of I5-1135G7@2.4Ghz, with 16 GB memory. Only thread parameters of the solver are modified to 4, while the other parameters are the default values. As long as the optimization gap settings are consistent, the third party will get the same results when using the above parameters for simulation.

3.1 Scenario 1

Scenario 1 is used to show the results of equipment layout under general constraints. We set the reliability thresholds $\mathrm{ASAI}^{\mathrm{lim}}$ and $\mathrm{SAIFI}^{\mathrm{lim}}$ to be 99.9% and 1.5 times/year, respectively. The optimization layout model in Eq. (34) is analysed and the optimal results are shown in Fig. 5.

There are a total of 6 fault indicators, 2 I-type switches and 5 V-type switches. ASAI is 99.94%, SAIFI is 1.19, $ELCC$ is ¥487,500, and CIC is ¥387,189. It can be seen that investing only ¥487,500 can improve ASAI by 1.09%, reduce SAIFI by 70.32%, and reduce CIC by 95%. Therefore, automatic transformation of the feeder is one of the most effective means to improve user perception of electricity consumption, and the quality and efficiency of power company operation.

3.2 Scenario 2

Scenario 2 is used to verify the rationality of the goal of minimizing the sum of equipment life cycle cost and customer interrupt cost. We set the reliability thresholds $\mathrm{ASAI}^{\mathrm{lim}}$ and $\mathrm{SAIFI}^{\mathrm{lim}}$ at 99.9% and 1.5 times/year, respectively. The results obtained based on Eq. (34) are shown in Table 3, with the respective goals of minimizing $ELCC$, CIC, and the sum of $ELCC$ and CIC.

According to Table 3, the following can be observed:

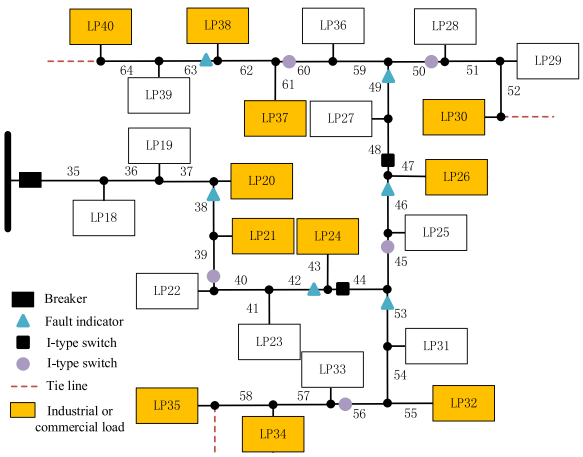

Fig. 5 Optimal layout results of scenario 1

(1) If the goal is to minimize *ELCC*, the reliability threshold is met by investing the least equipment, so the equipment life cycle cost is indeed the smallest. But because of the low reliability, the customer interrupt cost is the largest, which leads to a larger sum of ELCC and LCC.
(2) If the goal is to minimize *CIC*, as much equipment as possible will be installed to obtain the lowest customer interrupt cost and the highest reliability. But at the same time, the customer interrupt cost reduction due to the installed equipment is far less than the life cycle cost of the installed equipment itself. Consequently, it leads to the largest sum of *ELCC* and *LCC*.
(3) If the goal is to minimize the sum of *ELCC* and *LCC*, it will install a relatively large amount of equipment, so the reliability is slightly higher than the threshold. At the same time, the reduced customer interrupt cost is also considerably lower, resulting in the smallest sum of *ELCC* and *LCC*. Therefore, it is appropriate to take the minimum sum of *ELCC* and *LCC* as the optimization objective, and the results obtained have the lowest financial investment.

Table 4 Feature comparison of different schemes

Scheme	Fault indicator	I-type switch	V-type switch	Convex model
1	√			√
2		√		√
3			√	√
4	√	√		√
5	√		√	√
6		√	√	√
7	√	√	√	√
8	√	√	√	

$$T_i^{\text{patrol}} = \sum_{s\in\Omega_s} \frac{l_s}{v} \times \left(\left(1-\rho^{X_{i,s}+Z_{i,s}}\right) \times \prod_{n\in\Omega_{i,s}} (1-x_n)(1-z_n) + \rho^{X_{i,s}+Z_{i,s}} \right) \tag{35}$$

$$T_{i,j}^{\text{iso}} = t^{\text{iso}} \times \left(\left(1-p^{Y_{i,j}^i}\right) \times \prod_{n\in\Omega_{i,j}^i} (1-y_n) \right) + p^{Y_{i,j}^i} \tag{36}$$

$$T_{i,j}^{\text{outage}} = \left(\prod_{n\in\Omega_{i,j}^i} (1-y_n) \prod_{n\in\Omega_{i,j}} (1-z_m) \right) \times \left(t^{\text{loc}} + T_i^{\text{search}} + t^{\text{repair}} \right) + \left(1 - \prod_{n\in\Omega_{i,j}^i} (1-y_n) \prod_{n\in\Omega_{i,j}} (1-z_m) \right) \times T_{i,j}^{\text{iso}} \tag{37}$$

3.3 Scenario 3

Scenario 3 is used to verify the effectiveness of the optimal layout model while considering multiple types of equipment. The comparison scheme is designed as shown in Table 4.

In schemes 1–7, T_i^{patrol} is constructed by Eqs. (2)–(21), and $T_{i,j}^{\text{outage}}$ is constructed by Eqs. (22)–(27). So the constructed model is convex, where the global optimal solution can be obtained by branch and bound algorithm. For scheme 1, it only considers the installation of a fault indicator without other equipment, scheme 4 has a fault indicator and I-type switch, while scheme 6 has all three types of equipment at the same time. As the logic for other schemes is similar, they are not described further here.

In scheme 8, three types of equipment are considered at the same time, while T_i^{patrol} is constructed by Eq. (35) and $T_{i,j}^{\text{outage}}$ is constructed by Eqs. (36) and (37), as [19]:

where $T_{i,j}^{\text{iso}}$ is the isolation time for load j about fault i.

Further, based on Eq. (34) and ignoring the system average interruption duration index, aimed at minimizing equipment life cycle cost, the models corresponding to the above 8 schemes are analysed with ASAI^{lim} being 99.3%, 99.6% and 99.9%, respectively. In particular, for scheme 8, since it is a non-convex model, the solver in [19] needs to be used with all default parameter settings. All the solution results are shown in Tables 5, 6 and 7.

From the above results, the following observations can be made:

(1) When the reliability requirements are low, only a small number of fault indicators or I-type switches are needed to meet the requirements. If only V-type switches can be installed, it will cause a waste of money. For example, when ASAI^{lim} is 99.3%, the capital investment under scheme 6 is 400% of that for scheme 1, while reliability has not improved significantly.

Table 3 Comparison of results under different objectives

Minimize objective	*ELCC*/¥	*CIC*/¥	*ELCC* + *CIC*/¥	ASAI/%	SAIFI
ELCC	268,750	876,500	1,145,250	99.90	1.23
CIC	2,962,500	9131	2,971,631	99.99	0.0897
ELCC + *CIC*	487,500	387,189	874,689	99.94	1.19

Table 5 Solution results when $ASAI^{lim}$ is 99.3%

Scheme	Fault indicator	I-type switch	V-type switch	*ELCC*/¥	ASAI/%
1	3	0	0	18,750	99.30
2	0	1	0	37,500	99.30
3	0	0	1	75,000	99.31
4	3	0	0	18,750	99.30
5	3	0	0	18,750	99.30
6	0	1	0	37,500	99.30
7	3	0	0	18,750	99.30
8	4	0	0	25,000	99.91

Table 6 Solution results when $ASAI^{lim}$ is 99.6%

Scheme	Fault indicator	I-type switch	V-type switch	*ELCC*/¥	ASAI/%
1	29	0	0	181,250	99.60
2	0	5	0	187,500	99.60
3	0	0	2	150,000	99.60
4	3	1	0	56,250	99.61
5	1	0	1	81,250	99.60
6	0	1	1	112,500	99.65
7	3	1	0	56,250	99.61
8	0	1	1	112,500	99.63

Table 7 Solution results when $ASAI^{lim}$ is 99.9%

Scheme	Fault indicator	I-type switch	V-type switch	*ELCC*/¥	ASAI/%
1	–	–	–	–	–
2	–	–	–	–	–
3	0	0	5	375,000	99.91
4	–	–	–	–	–
5	10	0	3	287,500	99.90
6	0	1	4	337,500	99.90
7	7	2	2	268,750	99.90
8	6	1	3	300,000	99.91

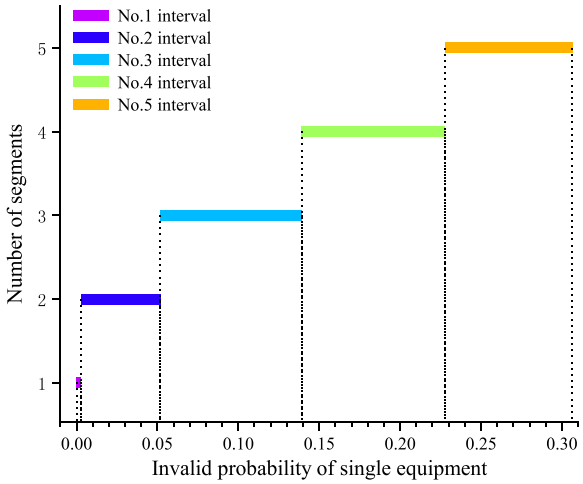

Fig. 6 The relationship between probability and segmentation

Table 8 Probability start and end points of each interval

Interval number	1	2	3	4	5
Start point	0	0.0027	0.0519	0.1392	0.2279
End point	0.0027	0.0519	0.1392	0.2279	0.3063

When the reliability requirements gradually increase, if only a single type of equipment is installed, none of the three types of equipment can meet the requirements with low capital investment, but if the cooperation relationship between equipment is considered, the requirements can be met with low capital investment, e.g., when $ASAI^{lim}$ is 99.6%, the capital investment under scheme 4 is much smaller than with other solutions.

As reliability requirements continue to rise, they cannot be met by a single type of equipment. However, with multiple types of equipment, the requirements can be met with minimal capital investment.

Therefore, it is most effective to consider multiple types of equipment at the same time. This can effectively improve reliability with minimal capital investment.

(2) From the results for scheme 8, it can be seen that the proposed model in this paper is a convex model, so a global optimal solution can be achieved. Therefore, compared with other, non-convex, models, it can also effectively save capital investment.

3.4 Scenario 4

Scenario 4 is used to verify the effectiveness of the 3δ principle and the proposed failure probability representation methods.

In this paper, the 3δ principle is used to describe the failure probability of multiple equipment through piecewise functions. From Eq. (8), it can be seen that the number of segments required for different failure probabilities is also different. Therefore, the failure probability is divided into several intervals according to the number of required segments, as shown in Fig. 6 and Table 8, where the failure probability is divided into 5 intervals.

Considering that the failure probability for equipment is generally lower than 20% [27], 4 segments are sufficient for most scenarios. At the same time, because the quantity of equipment is a discrete integer, there is another method to describe it as given by:

$$\varphi\left(\rho, X_{i,s}+Z_{i,s}\right)=\sum_{g=1}^{sum\left(\Omega_{i,s}\right)} b(g)\times\rho(g) \tag{38}$$

$$\sum_{g=1}^{sum\left(\Omega_{i,s}\right)} b(g)\times g=X_{i,s}+Z_{i,s} \tag{39}$$

$$\sum_{g=1}^{sum\left(\Omega_{i,s}\right)} b(g)=1 \tag{40}$$

In order to facilitate the comparison of the solution differences under different failure probability representation methods, the following definitions are made:

(1) Method C indicates that the failure probability of multiple equipment is set to the same constant as the failure probability of single equipment.
(2) Method A-n indicates that the failure probability of multiple equipment is represented by the piecewise function with the continuous domain defined by Eqs. (7)–(19), with G equal to n.
(3) Method B-n indicates that the failure probability of multiple equipment is represented by the piecewise function with the discrete domain defined by Eqs. (38)–(40), with G equal to n.
(4) Method B-S indicates that the failure probability of multiple equipment is represented by the piecewise function with the discrete domain defined by Eqs. (38)–(40), with G equal to $sum\left(\Omega_{i,s}\right)$.

Assuming that ρ equals 0.2 and $sum\left(\Omega_{i,s}\right)$ equals 7, the difference between the different methods is shown in Fig. 7.

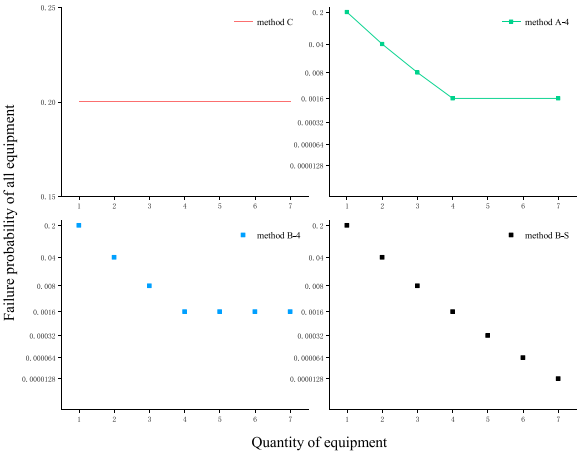

Fig. 7 The difference between different methods

From Fig. 7, it can be seen that:

(1) In method C, the failure probability of multiple equipment is constant and is the same as that for the failure probability of a single piece of equipment. It is too simple to be able reflect the objective logic that system reliability can be improved by increasing equipment redundancy.
(2) In method A-n, as the quantity of equipment increases, the failure probability of all equipment decreases, which conforms to the objective logic. Under the premise that the failure probability of single piece is 0.2, as long as the number of equipment pieces is greater than or equal to 4, the failure probability of all equipment is already lower than 0.0027, which satisfies the 3δ principle, so its change relationship can be represented through A-4.
(3) In method B-n, the change rule of the failure probability of multiple equipment is consistent with method A. When the amount of equipment is greater than 4 pieces, the failure probability of multiple equipment no longer changes. Although its expressions appear to be simpler than method A, since its domain is discrete, the number of segments reach $sum\left(\Omega_{i,s}\right)$, which varies with the topology. In particular, when the topology is complex, $sum\left(\Omega_{i,s}\right)$ is often greater than 4.
(4) In method B-S, the failure probability is exponentially related to the amount of equipment, which is the true failure probability.

Further, the failure probability of a single piece of equipment is set to 0.05, 0.1, 0.2 and 0.25, respectively, to compare the solution quality of different multi-equipment failure probability representation methods under

Table 9 Solution results when the failure probability of single equipment is 0.05

Method	Solve time/s	*ELCC*/¥	*CIC*/¥	Number of equipment		
				Fault indicator	I-type switch	V-type switch
C	24	1,037,500	229,964	4	9	9
A-2	184	993,750	235,695	3	10	8
B-2	289	993,750	235,695	3	10	8
B-S	607	993,750	234,455	3	10	8

Table 10 Solution results when the failure probability of single equipment is 0.1

Method	Solve time/s	*ELCC*/¥	*CIC*/¥	Number of equipment		
				Fault indicator	I-type switch	V-type switch
C	7	1,056,250	245,043	1	10	9
A-2	150	1,000,000	239,904	4	10	8
B-2	269	1,000,000	239,904	4	10	8
A-3	190	993,750	239,557	3	10	8
B-3	446	993,750	239,557	3	10	8
B-S	629	993,750	239,378	3	10	8

Table 11 Solution results when the failure probability of single equipment is 0.2

Method	Solve time/s	*ELCC*/¥	*CIC*/¥	Number of equipment		
				Fault indicator	I-type switch	V-type switch
C	5	1,068,750	279,332	3	10	9
A-2	270	1,043,750	235,482	5	11	8
B-2	415	1,043,750	235,482	5	11	8
A-3	305	1,012,500	238,841	6	10	8
B-3	750	1,012,500	238,841	6	10	8
A-4	365	1,006,250	240,347	5	10	8
B-4	812	1,006,250	240,347	5	10	8
B-S	975	1,006,250	240,310	5	10	8

different G values. Under the same functional failure probability of single equipment, all the involved examples have the same structure except for the multi-equipment failure probability representation method. The specific solution results are shown in Tables 9, 10, 11 and 12.

From the above results, it can be seen that:

(1) When the functional failure probability of multiple equipment is constant, the solution time is the shortest because of the simple structure. However, it ignores the fact that the actual failure probability of multiple equipment decreases with the increase of equipment quantity, resulting in excessive investment. At the same time, there may be unsolved situations such as in Table 12.

(2) Using method A-n or B-n to represent the functional failure probability of multiple equipment, its actual changing relationship can be fitted to a certain extent. Although auxiliary variables will reduce solution efficiency, the improvement of the solution quality reduces unnecessary capital investment.

(3) With the increase of segment number, the fitting of actual failure probability by method A-n or B-n gradually becomes accurate, so the required equipment life cycle cost is gradually reduced. From the results of method B-S, it is seen that it not only converges to the results of actual failure probability within the corresponding number of segments in Fig. 6, but also is much less time-consuming.

(4) Although the calculation accuracies of method A-n and B-n are consistent, method B-n introduces more auxiliary variables, resulting in obviously slower solution efficiency.

Therefore, it is reasonable and effective to describe the functional failure probability of equipment by means of piecewise functions in accordance with the 3δ principle, which can effectively reduce the equipment life cycle cost, the investment pressure of the power company, and the calculation time, and ensure calculation accuracy.

3.5 Scenario 5

Scenario 5 is used to show the difference and connection between patrol and power outage time. In order to compare these times under different reliability constraints, based on Eq. (34) and ignoring the system average interruption duration index, *ELCC* is minimized with $ASAI^{\lim}$ set as 99.9% and 99.99%, respectively. Considering that patrol and power outage time are longer when the reliability constraint is lower, taking patrol and power outage time corresponding to the threshold value of 99.9% minus patrol and power outage time corresponding to the threshold value of 99.99%, different results are obtained and shown in Fig. 8.

It can be seen that for patrol time, no fault will decrease its patrol time as reliability threshold increases, such as faults 49 and 50 and 59 to 63. For power outage time, there may be a long patrol time at a fault point, but the resulting power outage time is short, such as faults 49 and 59. This is because the

Table 12 Solution results when the failure probability of single equipment is 0.25

Method	Solve time/s	*ELCC*/¥	*CIC*/¥	Number of equipment		
				Fault indicator	I-type switch	V-type switch
C	–	–	–	–	–	–
A-2	231	1,031,250	264,140	3	11	8
B-2	350	1,031,250	264,140	3	11	8
A-3	283	1,037,500	228,885	4	9	9
B-3	448	1,037,500	228,885	4	9	9
A-4	439	1,012,500	246,469	6	10	8
B-4	491	1,012,500	246,469	6	10	8
A-5	645	1,012,500	245,250	6	10	8
B-5	842	1,012,500	246,469	6	10	8
B-S	1054	1,012,500	244,783	6	10	8

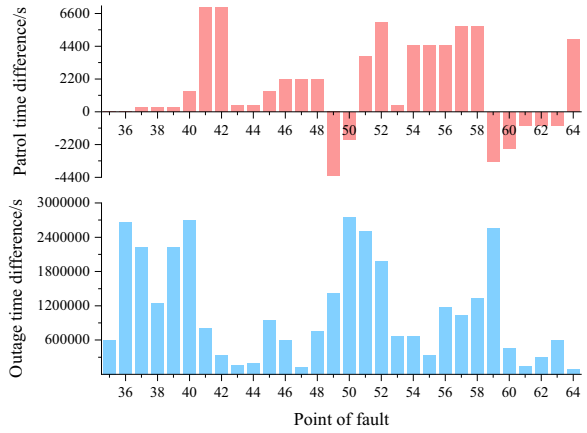

Fig. 8 Time difference comparison

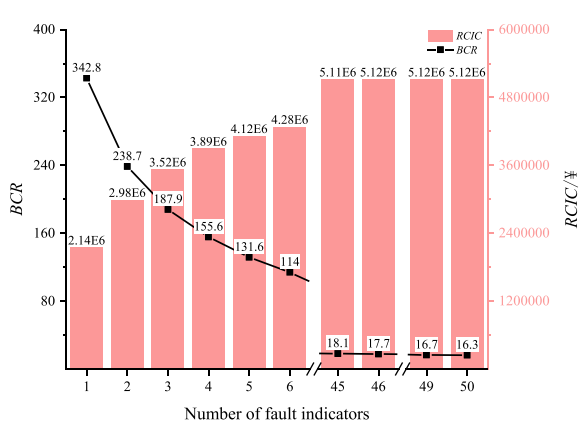

Fig. 9 *BCR* of fault indicator

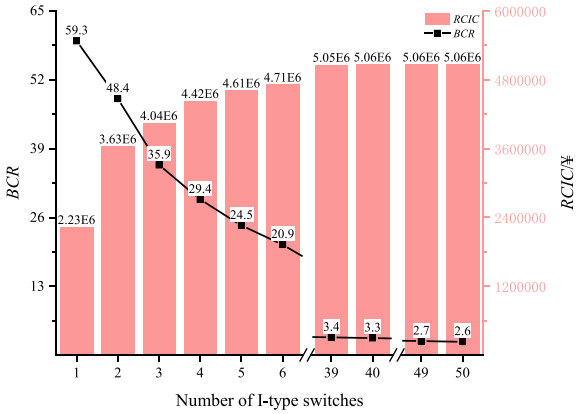

Fig. 10 *BCR* of I-type switch

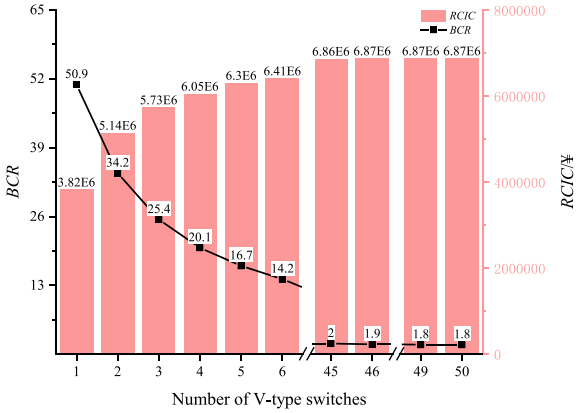

Fig. 11 *BCR* of V-type switch

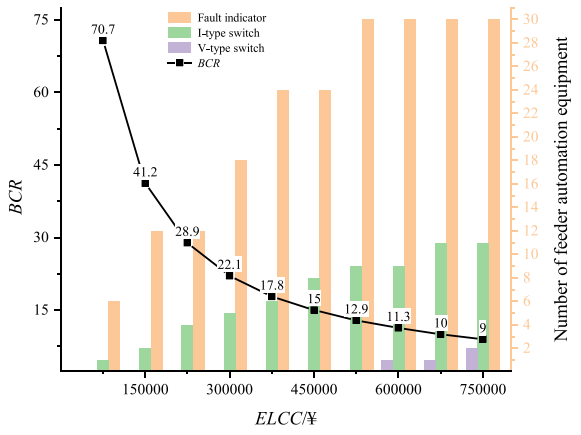

Fig. 12 *BCR* under different *ELCC*

isolation level of faults is different under different reliability constraints. The above results prove that it is reasonable to consider multiple types of equipment at the same time in the optimization process.

3.6 Scenario 6

Scenario 6 is used to demonstrate the benefits of different types of equipment.

The customer interruption cost can be effectively reduced by configuring feeder automation equipment. In order to better measure the relationship between the two, the reduced customer interruption cost (*RCIC*) is defined as the benefit, and the *ELCC* of equipment is defined as the cost, while the benefit cost ratio is further defined as *BCR*. The calculation example in this scenario is based on Eq. (34), while ignoring the supply reliability and minimizing *CIC*. With the quantity of equipment as a constraint, the *BCR* under different amounts of equipment is shown in Figs. 9, 10 and 11.

As shown, as the quantity of equipment increases, *BCR* gradually increases, but the value of the increase gradually decreases. For fault indicator and V-type switches, when the quantity is greater than 46, the benefits will not increase further. For the I-type switch, it starts to saturate after the quantity reaches 40.

The switch can obtain a maximum benefit of about ¥3,820,000, but due to its own high cost, the maximum *BCR* is only 50.9. For a single fault indicator, although the maximum benefit can only be ¥2,140,000, due to its low cost, its *BCR* is 343, which is much higher than the other two.

This scenario is further based on Eq. (34) while ignoring reliability, minimizing *CIC*, and optimizing the placement of three types of equipment at the same time with the *ELCC* as a constraint. The *ELCC* of a single V-type switch is used as the iteration gap, and the results shown in Fig. 12 are obtained by solving 10 times.

Because of the higher cost, although the V-type switch can greatly reduce the interruption cost for customers, it needs to wait until *ELCC* constraints are high before it is put into use. When the *ELCC* is constrained to be ¥75,000 there are a total of 6 fault indicators and 1 I-type switch, and the maximum benefit reaches about ¥5,300,000. Comparing Figs. 9 and 10, it can be seen that the benefit is higher than fault indicators or I-switches all configured.

The above results also show that by configuring multiple types of feeder automation equipment, the large interruption cost can be reduced at small cost.

4 Conclusions

Based on the explicit expression between power outage time and equipment layout, this paper proposes an optimal layout model of feeder automation equipment oriented to the type of fault detection and local action. It considers both the cooperation relationship of multiple types of equipment and the functional failure probability. As a convex model, the developed model can accurately solve the minimum economic investment required to meet relevant reliability constraints, conform to the actual production experience, and effectively help power company operational quality and efficiency, and customer perception of electricity consumption.

The analysis logic of power outage time in this paper is also applicable to the station-centralized feeder automation mode. However, it has certain limitations in the objective fact as random fluctuations in failure probability are not considered. Subsequent work will further advance towards examining stochastic failure probability.

Abbreviations

FLSR: Fault Location and Service Restore; ELCC: Equipment Life Cycle Cost; CIC: Customer Interrupt Cost; ASAI: Average Service Availability Index; SAIFI: System Average Interruption Frequency Index; RCIC: Reduced Customer Interrupt Cost; BCR: Benefit Cost Ratio.

Acknowledgements

Not applicable.

Author contributions

RC is responsible for optimizing model construction, XL is responsible for paper writing, and YC is responsible for guiding experimental ideas. All authors read and approved the final manuscript.

Funding

This work was supported by the National Natural Science Foundation of China (Grant No. 51777067).

Availability of data and materials

All data generated or analyzed during this study are included in the revised manuscript.

Declarations

Competing interests

We have no known competing financial interests or personal relationships that could have appeared to influence the work reported in this paper.

Author details

[1]Bishan Power Supply Branch of Chongqing Electric Power Company, Chongqing, Bishan, China. [2]North China Electric Power University, Beijing, China.

Received: 15 May 2022 Accepted: 27 December 2022
Published online: 12 January 2023

References

1. Zidan, A., Khairalla, M., Abdrabou, A. M., et al. (2016). Fault detection, isolation, and service restoration in distribution systems: State-of-the-art and future trends. *IEEE Transactions on Smart Grid, 8*(5), 2170–2185.
2. Chen, Y., Wu, C., & Qi, J. (2021). Data-driven power flow method based on exact linear regression equations. *Journal of Modern Power Systems and Clean Energy, 10*(3), 800–804.
3. Zhang, Z., Chen, Y., Ma, J., et al. (2022). Stochastic optimal dispatch of combined heat and power integrated AA-CAES power station considering thermal inertia of DHN. *International Journal of Electrical Power & Energy Systems, 141*, 108151.

4. Li, Z. X., Wan, J. L., Wang, P. F., et al. (2021). A novel fault section locating method based on distance matching degree in distribution network. *Protection and Control of Modern Power Systems, 6*(2), 253–263.
5. Li, C. C., Xi, Y. N., Lu, Y. F., et al. (2022). Resilient outage recovery of a distribution system: Co-optimizing mobile power sources with network structure. *Protection and Control of Modern Power Systems, 7*(3), 459–471.
6. Yin, X., Jinghan, H., Ying, W., et al. (2019). A review on distribution system restoration for resilience enhancement. *Transactions of China Electrotechnical Society, 34*(16), 3416–3429.
7. Shouxiang, W., Qi, L., Qianyu, Z., et al. (2021). Connotation analysis and prospect of distribution network elasticity. *Automation of Electric Power Systems, 45*(9), 1–9.
8. Kiaei, I., & Lotfifard, S. (2019). Fault section identification in smart distribution systems using multi-source data based on fuzzy petri nets. *IEEE Transactions on Smart Grid, 11*(1), 74–83.
9. Fereidunian, A., & Talabari, M. A. (2020). Service restoration enhancement by FIs deployment in distribution system considering available AMI system. *IET Generation, Transmission & Distribution, 14*(18), 3665–3672.
10. Cai, C., Ding, J., Lü, F., et al. (2020). Optimal placement of fault indicators based on integer linear programming model in distribution network. *Power System Protection and Control, 48*(1), 172–180.
11. He, L., He, B., Xu, J., et al. (2020). Optimal placement method of fault indicator in distribution network considering reliability constraints. *Automation of Electric Power Systems, 44*(18), 116–123.
12. Zhuangzhi, G., Qixing, X., Junjie, H., et al. (2017). Integer linear programming based fault section diagnosis method with high fault-tolerance and fast performance for distribution network. *Proceedings of the CSEE, 37*(3), 786–794.
13. He, R., Hu, Z., Li, Y., et al. (2018). Fault section location method for DG-DNs based on integer linear programming. *Power System Technology, 42*(11), 3684–3690.
14. Sun, L., Yang, H., & Ding, M. (2018). Mixed integer linear programming model of optimal placement for switching devices in distribution system. *Automation of Electric Power Systems, 42*(16), 87–95.
15. Zhang, T., Wang, C., Luo, F., et al. (2019). Optimal design of the sectional switch and tie line for the distribution network based on the fault incidence matrix. *IEEE Transactions on Power Systems, 34*(6), 4869–4879.
16. Farajollahi, M., Fotuhi-Firuzabad, M., & Safdarian, A. (2017). Optimal placement of sectionalizing switch considering switch malfunction probability. *IEEE Transactions on Smart Grid, 10*(1), 403–413.
17. Chen, B., Chen, H., & Li, B. (2019). Optimal planning of automatic switches in resilient distribution network against extreme disasters. *Electric Power Automation Equipment, 39*(11), 87–95.
18. Bian, Y., & Bie, Z. (2021). Resilience-enhanced optimal placement model of remote-controlled switch for smart distribution network. *Automation of Electric Power Systems, 45*(3), 33–39.
19. Wang, S., Liang, D., Ge, L., et al. (2016). Analytical FRTU deployment approach for reliability improvement of integrated cyber-physical distribution systems. *IET Generation, Transmission & Distribution, 10*(11), 2631–2639.
20. Liao, Y., Zhang, J., Wang, Z., et al. (2018). Three-stage optimization algorithm for the sectionalizing switch placement of a medium voltage overhead line. *Power System Technology, 42*(10), 3413–3419.
21. Lwin, M., Guo, J., Dimitrov, N., et al. (2018). Protective device and switch allocation for reliability optimization with distributed generators. *IEEE Transactions on Sustainable Energy, 10*(1), 449–458.
22. Liu, J., Cheng, H., & Zhang, Z. (2013). Planning of terminal unit amount in distribution automation systems. *Automation of Electric Power Systems, 37*(12), 44–50.
23. Liu, X., Wu, H., Li, Y., et al. (2020). A bi-level optimization model of distribution automation terminal configuration. *Power System Protection and Control, 48*(24), 136–144.
24. Ziyun, L., Lexiang, C., & Zizhen, W. (2016). A method of layout planning for distribution automation terminal. *Power System Technology, 40*(4), 1271–1276.
25. Farajollahi, M., Fotuhi-Firuzabad, M., & Safdarian, A. (2018). Simultaneous placement of fault indicator and sectionalizing switch in distribution networks. *IEEE Transactions on Smart Grid, 10*(2), 2278–2287.
26. Lü, X., Gao, H., Ye, S., et al. (2022). Intelligent terminal planning strategy considering reliability and economy reconfiguration for distribution network. *Proceedings of the CSEE, 42*(2), 589–602.
27. Liu, J., Zhang, Z., & Zhang, X. (2017). Investigation on fault processing for electric power distribution networks. *Power System Protection and Control, 45*(20), 1–6.
28. Billinton, R., & Jonnavithula, S. (1996). A test system for teaching overall power system reliability assessment. *IEEE Transactions on Power Systems, 11*(4), 1670–1676.